DESIGN OF A SWITCHED–RELUCTANCE MOTOR DRIVE FOR ELECTRIC PROPULSION

Second Annual Report – Part 3 (AR2.3)

Modeling and Nonlinear Control of a Switched Reluctance Motor To Minimize Torque Ripple

Zhen Zhong Ye, Terry W. Martin, Juan Carlos Balda

University of Arkansas
Department of Electrical Engineering
3217 Bell Engineering Center
Fayetteville, AR 72701 – 1201
(501) 575-3005

Prepared for

June 2000

20000710 097

Modeling and Nonlinear Control of a Switched Reluctance Motor to Minimize Torque Ripple

I. INTRODUCTION

The Second Annual Report has been divided into three parts in order to summarize the activities performed on this ONR grant from May 1, 1999, until May 31, 2000. The three parts are the following:

- Part 1 entitled "Modeling Switched Reluctance Motors under Multi-Phase Excitation" covers "modeling" activities performed under Task (b) - "Design of the SRM" – of this ONR Grant.
- Part 2 entitled "An Enhanced Simple Method for Designing Switched Reluctance Motors under Multi-Phase Excitation" covers "design" activities performed under Task (b) - "Design of the SRM" – of this ONR Grant.
- Part 3 entitled "Modeling and Nonlinear Control of a Switched Reluctance Motor to Minimize Torque Ripple" covers "control" activities performed under Task (c) - "Design of the SRM Converter" – of this ONR Grant.

The reminder of this report refers to Part 3 of the Second Annual Report.

The Switched Reluctance Motor (SRM) is suited for many variable speed and electric propulsion applications due to its simple and brushless structure and low cost. Its working principle is pretty simple; the torque is produced when current flows on a phase, and the rotor poles of a SRM are attracted towards the excited stator poles due to the tendency for the reluctance of the flux path to minimize. By sequentially exciting the stator-pole groups to attract rotor poles, continuous motion and continuous torque are achieved. However, due to the doubly salient construction and the commutation from one phase to the next one, torque ripple for this type of motor becomes an outstanding issue especially at low speeds, and hence it limits the SRM application as a servo drive. Torque ripple also brings up the issue of acoustic noise and vibrations. In the application of a SRM to electric propulsion, the objective is to get a smooth starting torque during the initial acceleration phase. There are two main approaches to reduce torque ripple, one is to improve the motor design by changing the stator and rotor structure while the other is on the basis of sophisticated control. However, control of a SRM is not easy due to its highly nonlinear electromagnetic properties and the coupling relationships among rotor position, current and torque. In this report, first, we derive a set of nonlinear equations under reasonable assumptions to characterize the inherent relationship among phase voltage, phase current, rotor position and developed instantaneous phase torque. Then, the control scheme for torque ripple minimization is proposed and described based on a torque controller and a fuzzy logic controller for adjusting turn-on and turn-off angles. Next, simulation results are analyzed for torque ripple minimization at different speeds to illustrate our approach. The relevant conclusions are finally given.

II. SRM NONLINEAR MODELING

In the following modeling it is assumed that no mutual magnetic coupling exists between the individual SRM phases. Since the inductance profile for each phase is periodic in nature, a Fourier Series representation can be used to express the phase inductance with respect to the rotor position [1], [2]

$$L(\theta, i) = L_0 + \sum_{n=1}^{\infty} L_n(i)\cos(nN_r\theta + \varphi_n)$$

where N_r is the number of rotor poles, i is the phase current, θ represents the rotor position, and φ_n stands for the phase angle of the nth harmonic component. Only the first four terms are considered and the following relevant assumptions are further made:

$$L_a(i) = L(0, i)$$
$$L_u(i) = L(\pi / N_r, i)$$
$$L_m(i) = L(\pi / 2N_r, i)$$
$$L_t(i) = L(\pi / 3N_r, i)$$

where $L_a(i)$, $L_u(i)$, $L_m(i)$, $L_t(i)$ are the aligned position inductance, the unaligned position inductance, the midway inductance, and the one-third-way inductance (from the aligned position), respectively. Then, the general expression of inductance for the SRM can be approximated as follows:

$$L = L_0(i) + \sum_{n=1}^{3} L_n(i)\cos(nN_r\theta) \qquad (1)$$

where,

$$L_0 = (1/4)(L_a + L_u) + (1/2)L_m$$
$$L_1 = (1/4)L_a - (1/2)L_m + (2/3)L_t - (5/12)L_u$$
$$L_2 = (1/4)(L_a + L_u) - (1/2)L_m$$
$$L_3 = (1/4)L_a + (1/2)L_m - (2/3)L_t - (1/12)L_u$$

In terms of the data directly obtained from measurements or Finite Element Analysis (FEA), we can fit the inductance curves $L_a(i)$, $L_m(i)$, $L_t(i)$, and $L_u(i)$ (see Fig.1) to get the analytical expressions given below:

$$
\begin{aligned}
L_a(i) &= a_{00} & (i<42A) \\
&= a_0 + a_1 i + a_2 i^2 & (42A \le i \le 135A) \\
L_m(i) &= b_{00} & (i<49A) \\
&= b_0 + b_1 i + b_2 i^2 & (49A \le i \le 135A) \\
L_t(i) &= c_{00} & (i<52A) \\
&= c_0 + c_1 i + c_2 i^2 & (52A \le i \le 135A) \\
L_u(i) &= d_0 & (0 \le i \le 135A)
\end{aligned}
$$

where,

$$a_{00} = 12.230 \ [mH]; \qquad a_0 = 16.284 \ [mH]$$
$$a_1 = -0.1040 \ [mH]; \qquad a_2 = 2.260 \times 10^{-4} \ [mH]$$
$$b_{00} = 6.063 \ [mH]; \qquad b_0 = 6.333 \ [mH]$$
$$b_1 = 1.151 \times 10^{-3} \ [mH]; \qquad b_2 = -1.225 \times 10^{-4} \ [mH]$$
$$c_{00} = 9.700 \ [mH]; \qquad c_0 = 8.770 \ [mH]$$
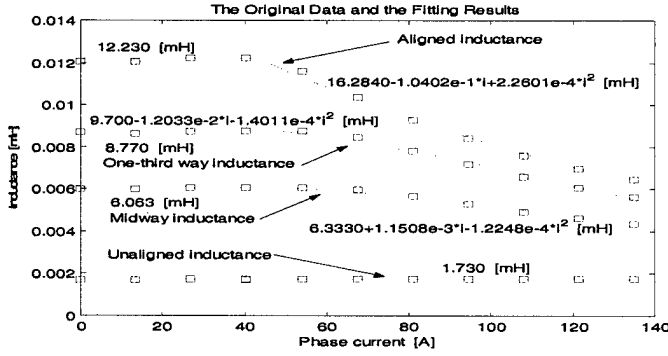$$c_1 = -1.203 \times 10^{-2} \ [mH]; \qquad c_2 = -1.40 \times 10^{-4} \ [mH]$$

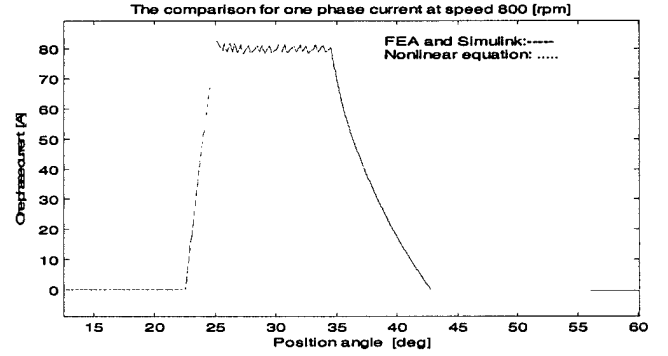Fig.1 The FEA original data and fitting results for a 10/8 SRM.

Fig.2 The comparison of current waveforms at n= 800 rpm.

$$d_0 = 1.730 \ [\text{mH}]$$

An analysis of Fig.1 shows that the four specific inductance curves are well fitted by the proposed expressions. According to electromagnetic theory, the back emf of one phase can be derived as follows:

$$
\begin{aligned}
e &= \frac{d\psi}{dt} = \frac{d(L \cdot i)}{dt} = L \cdot \frac{di}{dt} + i \cdot \frac{dL}{dt} \\
&= L \cdot \frac{di}{dt} + i \cdot \left(\frac{\partial L}{\partial \theta} \frac{d\theta}{dt} + \frac{\partial L}{\partial i} \frac{di}{dt} \right) \\
&= i\omega \cdot \frac{\partial L}{\partial \theta} + [L + i \cdot \frac{\partial L}{\partial i}] \cdot \frac{di}{dt}
\end{aligned}
\tag{2}
$$

where, ψ stands for the phase flux-linkage, ω is the rotor radian speed of the SRM. Therefore, the terminal voltage of that phase winding can be written as:

$$
u = Ri + e = [R + \omega \cdot \frac{\partial L}{\partial \theta}] \cdot i + [L + i \cdot \frac{\partial L}{\partial i}] \cdot \frac{di}{dt}
\tag{3}
$$

where R is the resistance of the phase winding. After some mathematical manipulations (see Appendix 1), we have:

$$
u = [R - \omega N_r \sum_{n=1}^{3} n \cdot L_n \cdot \sin(n \cdot N_r \theta)] \cdot i + [L_{01} + \sum_{n=1}^{3} L_{n1} \cos(n \cdot N_r \theta)] \cdot \frac{di}{dt}
\tag{4}
$$

where,

$$L_{01} = (1/4)(L_{a1} + L_{u1}) + (1/2)L_{m1}$$

$$L_{11} = (1/4)L_{a1} - (1/2)L_{m1} + (2/3)L_{t1} - (5/12)L_{u1}$$

$$L_{21} = (1/4)(L_{a1} + L_{u1}) - (1/2)L_{m1}$$

$$L_{31} = (1/4)L_{a1} + (1/2)L_{m1} - (2/3)L_{t1} - (1/12)L_{u1}$$

$$L_{a1} = a_0 + 2a_1 i + 3a_2 i^2$$

$$L_{m1} = b_0 + 2b_1 i + 3b_2 i^2$$

$$L_{t1} = c_0 + 2c_1 i + 3c_2 i^2$$

$$L_{u1} = d_0$$

The relationship between the terminal voltage and winding current is clearly described in the above equation, from which we find that each phase current not only depends on the phase terminal voltage but also on the rotor position. It is noted that the analytical solution of the phase current is almost unlikely because of this highly nonlinear equation. Fig.2 shows the effectiveness of this mathematical model when comparing phase current obtained from this model and that one using a MATLAB Simulink model together with FEA data.

The electromagnetic torque developed by one phase can be derived from the co-energy relations [11] as follows:

$$T = \frac{\partial W}{\partial \theta} = \frac{\partial \int_0^i \psi di}{\partial \theta} = \frac{\partial \int_0^i L \cdot i di}{\partial \theta} \tag{5}$$

where, W is the co-energy of that phase produced by the phase excitation. From Appendix 2, we directly have:

$$T = (-N_r i^2) \sum_{n=1}^{3} n \cdot L_{n2} \cdot \sin(n \cdot N_r \theta) \tag{6}$$

where,

$$L_{12} = (1/4)L_{a2} - (1/2)L_{m2} + (2/3)L_{t2} - (5/12)L_{u2}$$

$$L_{22} = (1/4)(L_{a2} + L_{u2}) - (1/2)L_{m2}$$

$$L_{32} = (1/4)L_{a2} + (1/2)L_{m2} - (2/3)L_{t2} - (1/12)L_{u2}$$

$$L_{a2} = (1/2)a_0 + (1/3)a_1 i + (1/4)a_2 i^2$$

$$L_{m2} = (1/2)b_0 + (1/3)b_1 i + (1/4)b_2 i^2$$

$$L_{t2} = (1/2)c_0 + (1/2)c_1 i + (1/3)c_2 i^2$$

$$L_{u2} = (1/2)d_0$$

It is straightforward that the phase torque equation is also a highly nonlinear function with respect to the rotor position and current. Fig.3 shows the normalized phase torque waveform of this 10/8 SRM versus current and rotor position, where the unaligned position is $(\frac{180}{N_r} \pm \frac{360k}{N_r})$ degree, k is an integer, and N_r is 5 for this specific case.

III.   TORQUE RIPPLE MINIMIZATION

The traditional approach for torque ripple reduction is based on the assumption of magnetic linearity so that the inductance versus angle variation is constant. In that case, the torque is supposed to be free of ripple if each phase current is designed to have a flat-top shape. However, a practical SRM is always designed with magnetic saturation in order to achieve better power/weight ratio. Thus, even if the current waveform has a flat top, there still exist instantaneous torque pulsations as shown in Fig.4.

Considering the spatial angular cycle $2\pi/5$ between phases of this 10/8 SRM as well as the assumption of negligible mutual inductance and losses, we have the following state-space equations for the SRM system:
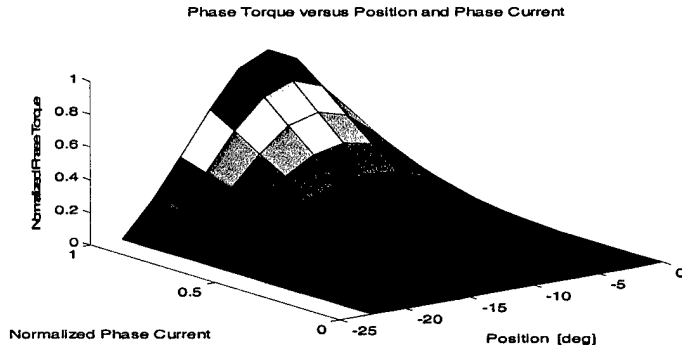
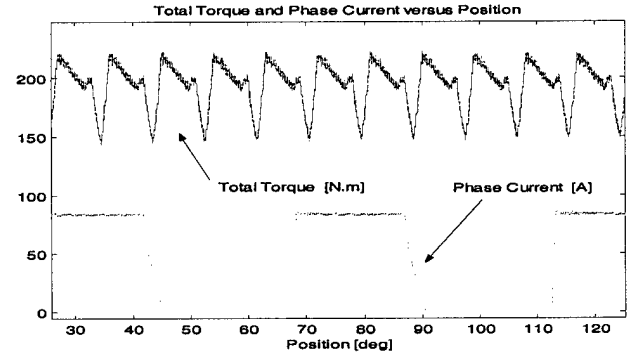Fig.3 The phase torque versus phase current and rotor position

Fig.4 The total torque and flat-top phase current.

$$\frac{di_j}{dt} = \mathsf{L_j}^{-1} (u_j - i_j \mathsf{R_j})$$

$$\frac{d\omega}{dt} = J^{-1} (T_{total} - T_L - B \cdot \omega)$$

$$\frac{d\theta}{dt} = \omega$$

$$T_{total} = \sum_{j=1}^{5} T_j$$

$$T_j = (-N_r i_j^{2}) \sum_{n=1}^{3} n \cdot L_{n2} \cdot \sin[n(N_r\theta - (j-1)\tfrac{2\pi}{5}]$$

where, $j = 1,2,...,5$, and,

u_j : The j-th phase voltage

i_j : The j-th phase current

$\mathsf{L_j}$: $L_{01} + \sum_{n=1}^{3} L_{n1} \cos[n \cdot (N_r\theta - (j-1)\tfrac{2\pi}{5})]$

$\mathsf{R_j}$: $R - \omega N_r \sum_{n=1}^{3} n \cdot L_n \cdot \sin[n \cdot (N_r\theta - (j-1)\tfrac{2\pi}{5})]$

B : Coefficient of viscous friction

J : Moment of inertia

T_L : Load torque

T_j : The j-th phase torque

T_{total} : Total electromagnetic torque

These equations are useful for theoretical analyses based on the SRM nonlinear model developed above. However, in a practical simulation or real-time implementation of torque control, even if there is an analytical expression for the phase torque, it is still unlikely to obtain the inverse expression for phase current in terms of the torque and rotor position from this nonlinear model. On the other hand, such a technique is more practical as a look-up table based interpolation (used in our simulations) or neural-network based estimation.
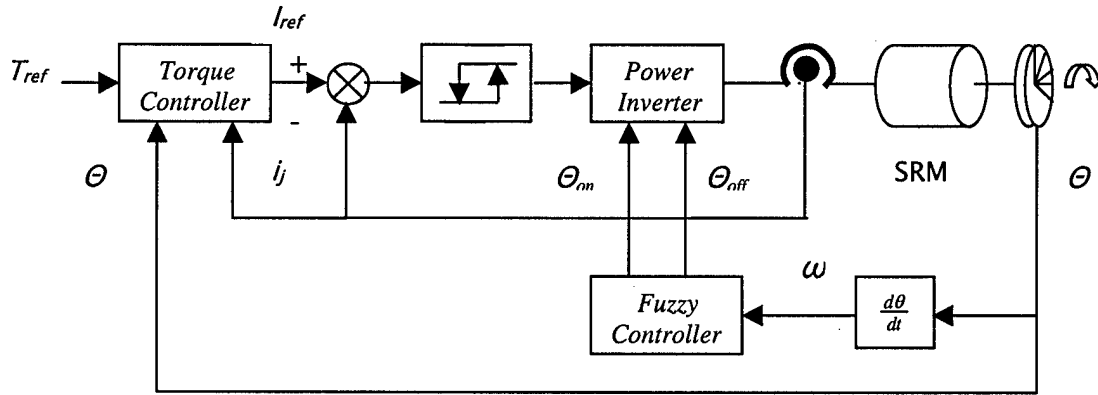
Fig.5 The control block diagram for the torque ripple minimization technique.

In terms of the torque expression $T_j (j = 1,2,...,5)$, we can find that, at any time instant, the total torque T_{total} of a SRM is dependent on the individual contribution of each phase torque T_j. If each phase torque can be controlled in real time according to the torque de-coupling requirement, then it is possible for the total torque of the SRM to track a torque command, and in turn, to minimize the instantaneous torque ripple.

As we already know, each phase torque varies with both the phase current and rotor position. In practice, there are four controllable parameters associated with current regulation if a current hysteresis-band controller is used in each phase. These are the reference phase current I_{ref}, the turn-on angle θ_{on}, the turn-off angle θ_{off}, and the current hysteresis bandwidth δI. Normally, δI is set constant for a specific application in terms of trade-off considerations between switching losses and current control accuracy. However, turn-on and turn-off angles along with the reference phase current directly determine the amount of current flowing into the phase winding, and in turn determine the produced torque. Therefore, these three parameters need to be adjusted in real time so as to indirectly regulate each phase torque, and accordingly, to control the instantaneous total torque T_{total}. It is not surprising that our torque ripple minimization work is based on this principle of indirect torque control in real time.

Moreover, we have to notice that the relationships between torque, current, speed, and firing angles are highly nonlinear; and that the controllable parameters vary with speed and load. Also, the final effect of torque ripple minimization is related to the torque reference command.

The control block of the whole system is shown in Fig.5. The torque controller uses measured phase current to estimate the torque produced by each phase based on a look-up table where $T_j = f(i_j, \theta - (j-1)\frac{2\pi}{5})$, then the torque command T_{ref} is de-coupled into the required phase torque reference T_{j_ref}. After that, in terms of the inverse relationship $i_j = g(T_j, \theta - (j-1)\frac{2\pi}{5})$, the torque controller calculates the phase reference current I_{j_ref} necessary to produce a desired phase torque. In practice, if the torque is already within the torque error band, then the phase reference current is kept at the same value as the previous one.

A fuzzy logic controller is designed for the regulation of θ_{on} and θ_{off}. The input variable to this controller is rotor speed n, which is defined to have a speed range of 0-6000 rpm for the SRM used in this research. Thus, its output after fuzzification is a fuzzy degree of membership. Similarly, if the unaligned and aligned positions are assumed to be $-22.5°$ and $0°$, respectively, then one output of the controller, turn-on angle θ_{on}, is defined as $-22.5° \sim -24.5°$, and the other output, turn-off angle θ_{off}, is within $0° \sim -15°$. Each variable is then divided into fuzzy regions as shown in Fig.6, 7, and 8. The variable spaces of rotor speed ω, turn-on angle θ_{on}, and turn-off angle θ_{off} are divided into 7, 3, and 5 regions, respectively. Each region is assigned a fuzzy membership function with triangular or trapezoidal shapes. We have the following rules for the fuzzy rule base:

If speed is s1, then turn-on is b, and turn-off is b2;
If speed is s2, then turn-on is m, and turn-off is b1;
If speed is m, then turn-on is s, and turn-off is m;
If speed is b1, then turn-on is s, and turn-off is m;
If speed is b2, then turn-on is s, and turn-off is s2;
If speed is b3, then turn-on is s, and turn-off is s1;
If speed is b4, then turn-on is s, and turn-off is s1;
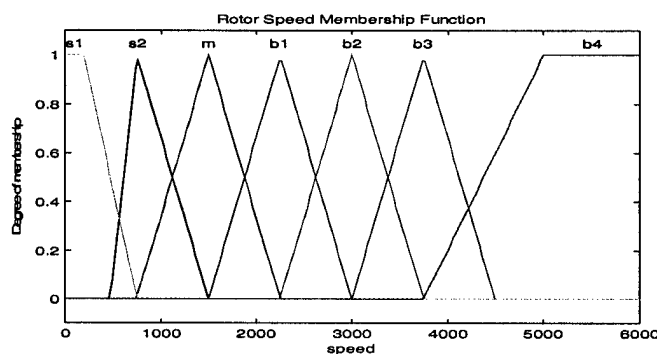

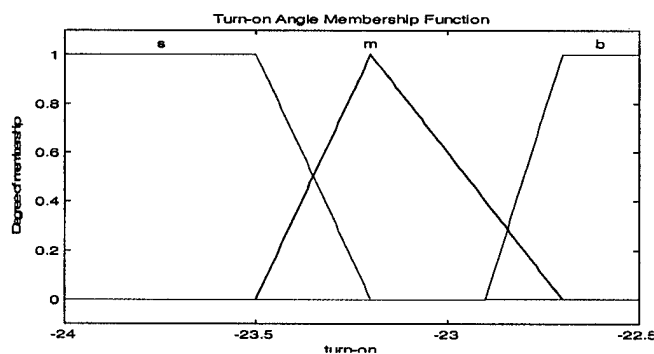Fig.6 The rotor speed membership function.
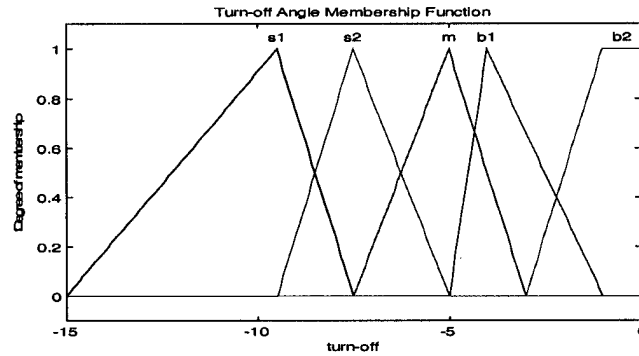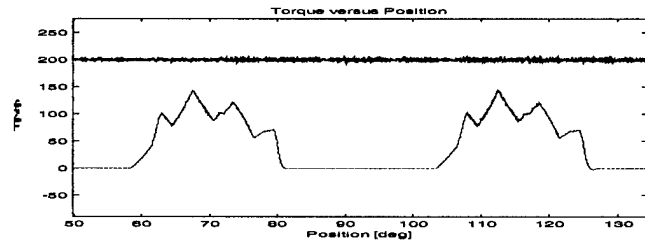

Fig.7 The turn-on angle membership function.

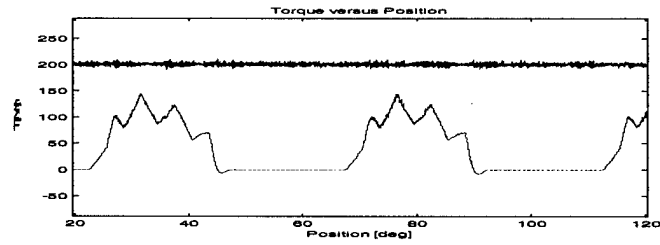Fig.8 The turn-off angle membership function.

In addition, implication is made for each rule in terms of the 'min' method, which truncates the output fuzzy set. However, the output of each rule based on the 'max' method, is aggregated into a single fuzzy set whose membership function assigns a weight for every output value. Finally, the defuzzification is implemented by means of the 'centroid calculation' method.
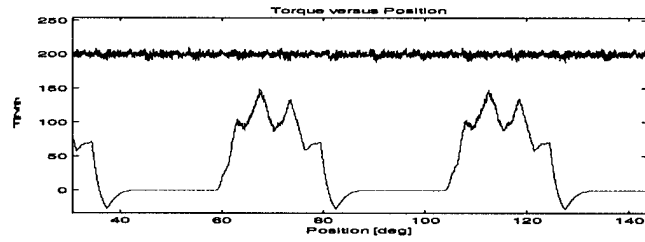
IV.   SIMULATION RESULTS

MATLAB Simulink based simulations with a step size of 1e-5 seconds were carried out for the 10/8 SRM, whose parameters are given in Appendix 3. Illustrative results can be found in Fig.9, 10, and 11. From Fig.9, we can see that the torque ripple is significantly reduced in the low-speed region up to 500 rpm within ± 5%. However, the torque ripple rises as the rotor speed increases.   At 1200 rpm, the ripple is ± 12% with respect to the torque command of 110 N.m, and at 4500 rpm, even that the torque command drops to 10 N.m, the torque ripple still increases up to ± 22%. A reasonable interpretation for this phenomenon is that the instantaneous phase current is unable to follow the desired reference current in the intermediate or high speed region since the rate of change of phase current rises rapidly as the rotor speed increases. On the other hand, we also realize that extending the commutation period may be beneficial to torque-ripple reduction as shown in Fig.10, especially in the intermediate speed region, and may boost the torque tracking capability to a higher level along with minimized torque ripple. In this case, negative instantaneous phase torque may occur and thus reduce the system efficiency. Finally, the torque step response of this SRM system at a rotor speed of 300 rpm is shown in Fig.11, where the torque command jumps from 120 N.m to 200 N.m, and then back to 120 N.m. The instantaneous torque still follows the command well and the torque ripple is limited to ± 4% of the command value.
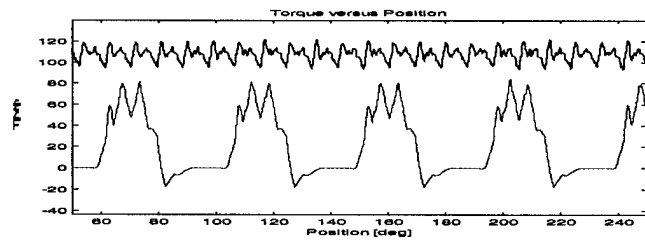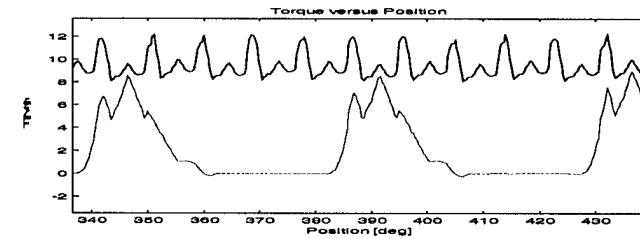
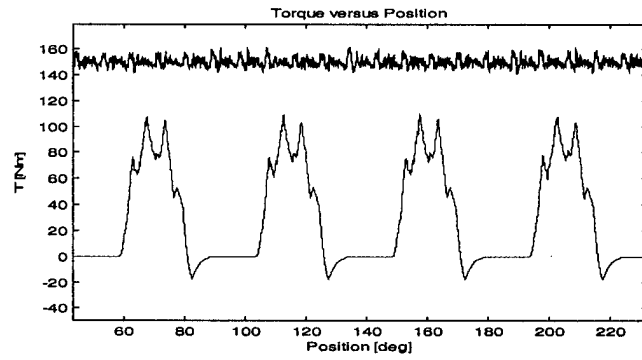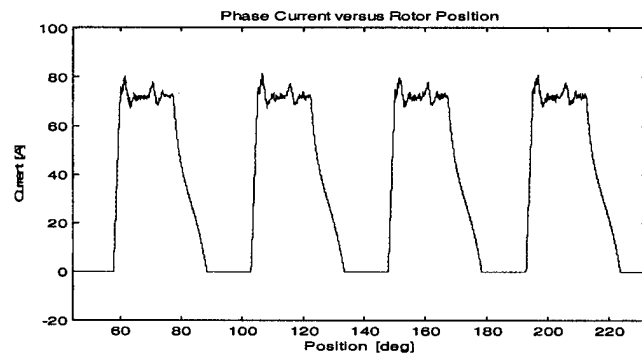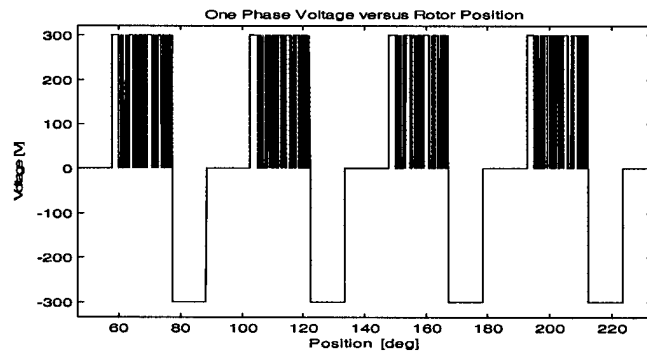Fig.9   The waveforms of instantaneous total torque T_{total} (top graph) and phase torque T_j (bottom graph);
(a) $T_{ref} = 200N.m$,   n = 10 rpm;   (b) T_{ref} = 200N.m ,   n = 200 rpm;   (c) T_{ref} = 200N.m,   n = 500 rpm;
(d) T_{ref}=110N.m , n = 1200 rpm (the rated speed of the specific SRM);   and (e) T_{ref} = 10N.m , n = 4500 rpm.

(a)

(b)

(c)

Fig.10   Waveforms of (a) instantaneous torque T_{total} (top graph) and phase torque T_j (bottom graph) at n= 800 rpm, T_{ref} = 150 N.m ; (b) phase current ; (c) phase voltage.
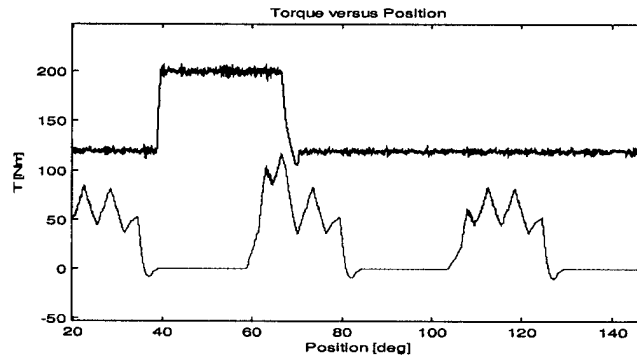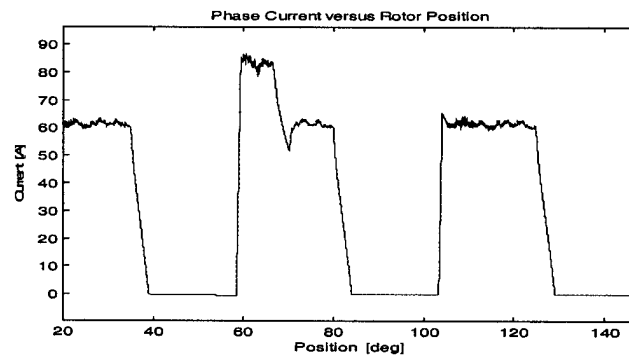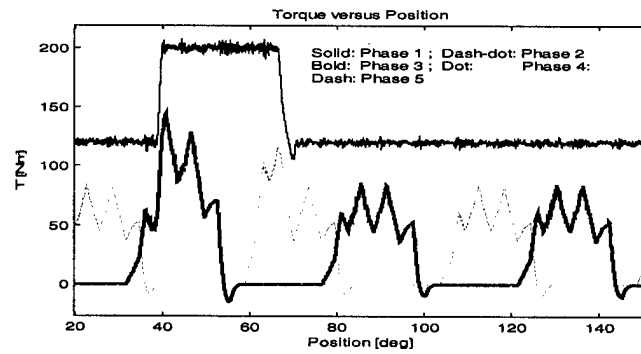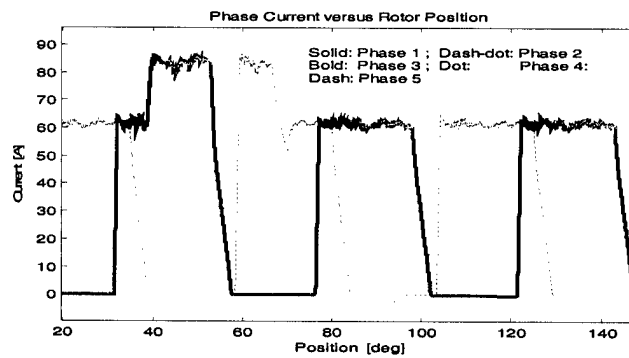
Fig.11 The step response waveforms of (a) instantaneous torque T_{total} (top graph) and phase torque T_1 (bottom graph) at n = 300 rpm, T_{ref} jumps from 120 N.m to 200 N.m, then back to 120 N.m; (b) the current of phase 1; (c) each phase torque; and (d) each phase current.

IV. CONCLUSIONS

This report proposed a nonlinear mathematical model for a 10/8 SRM in terms of a Fourier Series expression of the phase self-inductance. A torque ripple minimization technique based on indirect dynamic torque control was introduced. A corresponding control block based on a torque controller (for regulating the phase reference current) and a fuzzy logic controller (for adjusting the turn-on and turn-off angles) was described. Simulation results showed the feasibility of the developed approach to minimize the torque ripple, especially in the low-speed region. However, as the SRM operates in the high-speed region, the rate of change of the phase current limits any torque-ripple improvement. On the other hand, extending the phase commutation period to allow for negative torque may be beneficial to minimize the torque ripple.

REFERENCES

[1] B. Fahimi, G. Suresh, J. Mahdavi, M. Ehsani, "A new approach to model switched reluctance motor drive application to dynamic performance prediction, control, and design", *IEEE PESC'98,* Fukuoka, Japan, pp.2097-2102.

[2] J. Mahdavi, G. Suresh, B. Fahimi, M. Ehsani, "Dynamic modelling of nonlinear SRM drive with PSpice", *IEEE IAS 1997 Annual Meeting*, New Orleans, October 1997, pp. 661-667.

[3] M. Ilic-Spong, T. J. E. Miller, S. R. MacMinn, J. S. Thorp, "Instantaneous Torque Control of Electric Motor Drives", *IEEE Transactions on Power Electronics*, Vol.2, No.1, January 1987, pp.55-61.

[4] F. Filicori, C. Guarino Lo Bianco, A. Tonielli, "Modelling and Control Strategies for a Variable Reluctance Direct-Drive Motor", *IEEE Transactions on Industrial Electronics,* Vol.40, No.1, February 1993, pp.105-115.

[5] R. S. Wallace, D. G. Taylor, "A Balanced Commutator for Switched Reluctance Motor to Reduce Torque Ripple", *IEEE Transactions on Power Electronics*, Vol.7, N0.4, October 1992, pp.617-626.

[6] M. Ilic-Spong, R. Marino, S.Persada, D.G.Taylor, "Feedback Linearizing Control of Switched Reluctance Machines", *IEEE Transactions on Automatic Control,* Vol.AC-32, No.5, May 1987, pp.371-379.

[7] D. S. Schramm, B. W. Williams, T. C. Green, "Optimum Commutation Current Profile on Torque Linearization of Switched Reluctance Motors", *Proceedings of ICEM* 1992, pp.484-488.

[8] I. Husain, M. Ehsani, "Torque Ripple Minimization in Switched Reluctance Motor Drives by PWM Current Control", *IEEE APEC 1994*, pp.72-77.

[9] K. Russa, I. Husain, M. Elbuluk, "Torque Ripple Minimization in Switched Reluctance Machines over Wide Speed Range", *IEEE IAS 1997 Annual Meeting*, pp.668-675.

[10 P.C. Kjaer, J. J. Gribble, T.J.E. Miller, "High Grade Control of Switched Reluctance Machines", *IEEE IAS 1996 Annual Meeting*, pp.92-100.

[11] T. J. E. Miller, Switched Reluctance Motors and their Control, Magna Physics Publishing and Clarendon Press Oxford, 1993

APPENDIX 1

Let the generalized forms for $L_a(i), L_u(i),\ L_m(i),\ L_t(i)$ be as follows,

$$L_a(i) = \sum_{n=0} a_n i^n$$

$$L_m(i) = \sum_{n=0} b_n i^n$$

$$L_t(i) = \sum_{n=0} c_n i^n$$

$$L_u(i) = d_0$$

In terms of the inductance equation *(1)*, we then have,

$$\frac{\partial L}{\partial \theta} = \frac{\partial[L_0 + \sum_{n=1} L_n \cos(nN_r\theta)]}{\partial \theta}$$

$$= (-N_r)\sum_{n=1} L_n \cdot n \cdot \sin(nN_r\theta) \qquad (A-1)$$

$$L + i \cdot \frac{\partial L}{\partial i} = L_0 + \sum_{n=1} L_n \cos(nN_r\theta) + i \cdot \left(\frac{\partial[L_0 + \sum_{n=1} L_n \cos(nN_r\theta)]}{\partial i}\right)$$

$$= L_0 + \sum_{n=1} L_n \cos(nN_r\theta) + \left(i\frac{\partial L_0}{\partial i} + \sum_{n=1} i\frac{\partial L_n}{\partial i}\cos(nN_r\theta)\right)$$

$$= (L_0 + i\frac{\partial L_0}{\partial i}) + \sum_{n=1}(L_n + i\frac{\partial L_n}{\partial i})\cos(nN_r\theta)$$

$$= L_{01} + \sum_{n=1} L_{n1} \cos(nN_r\theta) \qquad (A-2)$$

where we denote $L_{01}(i),\ L_{11}(i),\ L_{21}(i),\ L_{31}(i)$ as

$$L_{01} = (L_0 + i\frac{\partial L_0}{\partial i})$$

$$= [(1/4)(L_a + i\frac{\partial L_a}{\partial i}) + (1/4)(L_u + i\frac{\partial L_u}{\partial i}) + (1/2)(L_m + i\frac{\partial L_m}{\partial i})]$$

$$= [(1/4)(\sum_{n=0}(n+1)a_n i^n) + (1/4)(d_0) + (1/2)(\sum_{n=0}(n+1)b_n i^n)]$$

$$= (1/4)(L_{a1} + L_{u1}) + (1/2)L_{m1}$$

where,

$$L_{a1} = \sum_{n=0}(n+1)a^n i^n$$

$$L_{m1} = \sum_{n=0}(n+1)b^n i^n$$

$$L_{u1} = d_0$$

On the other hand,

$$L_{11} = (L_1 + i\frac{\partial L_1}{\partial i})$$

$$= [(1/4)(L_a + i\tfrac{\partial L_a}{\partial i}) - (5/12)(L_u + i\tfrac{\partial L_u}{\partial i}) -$$
$$- (1/2)(L_m + i\tfrac{\partial L_m}{\partial i}) + (2/3)(L_t + i\tfrac{\partial L_t}{\partial i})]$$
$$= (1/4)L_{a1} - (5/12)L_{u1} - (1/2)L_{m1} + (2/3)L_{t1}$$

where,

$$L_{t1} = \sum_{n=0} (n+1)c_n i^n$$

Similarly, we can get the expressions for L_{21} and L_{31} as indicated before. According to the expressions *(3)*, *(A-1)* and *(A-2)*, it follows that the terminal voltage expression for one phase can be derived as shown in *(4)*.

APPENDIX 2

In terms of (5), we have,

$$T = \frac{\partial \int_0^i L \cdot i \, di}{\partial \theta}$$

$$= \frac{\partial \int_0^i (L_0 + \sum_{n=1} L_n \cos(nN_r \theta)) \cdot i \, di}{\partial \theta}$$

$$= \frac{\partial \int_0^i (\sum_{n=1} L_n \cos(nN_r \theta)) \cdot i \, di}{\partial \theta}$$

$$= \sum_{n=1} \int_0^i i \cdot L_n \cdot \frac{\partial \cos(nN_r \theta)}{\partial \theta} \cdot di$$

$$= (-N_r) \sum_{n=1} [n \cdot \sin(nN_r \theta) \cdot (\int_0^i i \cdot L_n di)] \qquad (A-3)$$

Since L_n (n=1,2,3) is a linear combination of L_a, L_m, L_t and L_u, and without losing generality, we assume:

$$L_n = K_{na} L_a + K_{nm} L_m + K_{nt} L_t + K_{nu} L_u$$

where, K_{na}, K_{nm}, K_{nt} and K_{nu} are individual coefficients. Therefore,

$$\int_0^i i \cdot L_n di = \int_0^i (K_{na} i L_a + K_{nm} i L_m + K_{nt} i L_t + K_{nu} i L_u) di$$

$$= K_{na} \sum_{n=0} \int_0^i a_n i^{n+1} di + K_{nm} \sum_{n=0} \int_0^i b_n i^{n+1} di + K_{nt} \sum_{n=0} \int_0^i c_n i^{n+1} di + K_{nu} \int_0^i d_0 i \, di$$

$$= K_{na}i^2 \cdot \sum_{n=0} \tfrac{a_n}{n+2} \cdot i^n + K_{nm}i^2 \cdot \sum_{n=0} \tfrac{b_n}{n+2} \cdot i^n + K_{nt}i^2 \cdot \sum_{n=0} \tfrac{c_n}{n+2} \cdot i^n + K_{nu}i^2 \cdot d_0 \cdot (\tfrac{1}{2})$$

$$= i^2 [K_{na}L_{a2} + K_{nm}L_{m2} + K_{nt}L_{t2} + K_{nu}L_{u2}]$$

$$= i^2 \cdot L_{n2} \qquad\qquad (A-4)$$

where,

$$L_{n2} = [K_{na}L_{a2} + K_{nm}L_{m2} + K_{nt}L_{t2} + K_{nu}L_{u2}]$$

$$L_{a2} = \sum_{n=0} \tfrac{a_n}{n+2} \cdot i^n = (1/2)a_0 + (1/3)a_1 i + (1/4)a_2 i^2$$

$$L_{m2} = \sum_{n=0} \tfrac{b_n}{n+2} \cdot i^n = (1/2)b_0 + (1/3)b_1 i + (1/4)b_2 i^2$$

$$L_{t2} = \sum_{n=0} \tfrac{c_n}{n+2} \cdot i^n = (1/2)c_0 + (1/3)c_1 i + (1/4)c_2 i^2$$

$$L_{u2} = (1/2)d_0$$

If we substitute the individual coefficients of L_1, L_2 and L_3 for K_{nm}, K_{nt} and K_{nu}, respectively, it is straight forward that the expressions for L_{12}, L_{22} and L_{32} are exactly the same as those shown before. In addition, in terms of *(A-3)*, the torque developed by one phase is given by

$$T = (-N_r)\sum_{n=1} [n \cdot \sin(nN_r\theta) \cdot (i^2 L_{n2})]$$

$$= (-N_r i^2)\sum_{n=1} [n \cdot \sin(nN_r\theta) \cdot L_{n2}]$$

as indicated in *(6)*.

APPENDIX 3

Main parameters of the simulated SRM
Number of stator poles: 10
Number of rotor poles: 8
Rated speed: 1200 rpm
Maximum designed speed: 6000 rpm
DC link voltage: 300V
Rated Current: 120A
Phase resistance: 0.082 Ω
Unaligned Inductance: 1.730 mH
Maximum aligned inductance: 12.23 mH.

REPORT DOCUMENTATION PAGE

Public reporting burden for this collection of information is estimated to average 1 hour per response, including the time for reviewing instructions, searching existing data sources, gathering and maintaining the data needed, and completing and reviewing the collection of information. Send comments regarding this burden estimate or any other aspect of this collection of information, including suggestions for reducing this burden to Washington Headquarters Services, Directorate for Information Operations and Reports, 1215 Jefferson Davis Highway, Suite 1204, Arlington, VA 22202-4302, and to the Office of Management and Budget, Paperwork Reduction Project (0704-0188), Washington, DC 20503.

1. AGENCY USE ONLY *(Leave blank)*	2. REPORT DATE June 2000	3. REPORT TYPE AND DATES COVERED Annual report (Pt.3), 5/1/99 - 5/30/00

4. TITLE AND SUBTITLE Second Annual Report - Part 3 (AR2.3) Modeling and Nonlinear Control of a Switched Reluctance Motor to Minimize Torque Ripple	5. FUNDING NUMBERS G 00014-98-1-0617 PR 98PRO5665-00

6. AUTHOR(S)

Zhen Zhong Ye, Terry W. Martin, Juan Carlos Balda

7. PERFORMING ORGANIZATION NAMES(S) AND ADDRESS(ES) University of Arkansas, Office of Research and Sponsored Programs, 120 Ozark Hall, Fayetteville, AR 72701	8. PERFORMING ORGANIZATION REPORT NUMBER AR2.3

9. SPONSORING / MONITORING AGENCY NAMES(S) AND ADDRESS(ES) Office of Naval Research ONR 242 Ballston Centre Tower One, 800 North Quincy Street, Arlington, VA 22217-5660	10. SPONSORING / MONITORING AGENCY REPORT NUMBER

11. SUPPLEMENTARY NOTES

a. DISTRIBUTION / AVAILABILITY STATEMENT APPROVED FOR PUBLIC RELEASE	12. DISTRIBUTION CODE

13. ABSTRACT *(Maximum 200 words)*

Part 3 of 3 of the Second Annual Report covers "control" activities performed under Task (c) - "Design of the SRM Converter" of this ONR Grant. The activities were performed from 5/1/99 to 5/30/00. This report, first, derives a set of nonlinear equationsto characterize the inherent relationship among phase voltage, phase current, rotor position and instantaneous phase torque. Then, the report proposes a control scheme for torque ripple minimization based on a torque controller. Next, it describes a fuzzy logic controller to adjust the turn-on and turn-off angles. Finally, simulation results are evaluated at different rotor speeds to illustrate the feasibility of the proposed ideas.

14. SUBJECT TERMS Annual report, main activities	15. NUMBER OF PAGES 16
	16. PRICE CODE

17. SECURITY CLASSIFICATION OF REPORT UNCLASSIFIED	18. SECURITY CLASSIFICATION OF THIS PAGE UNCLASSIFIED	19. SECURITY CLASSIFICATION OF ABSTRACT UNCLASSIFIED	20. LIMITATION OF ABSTRACT UL